

Cite this: *Chem. Commun.*, 2012, **48**, 4902–4904

www.rsc.org/chemcomm

## COMMUNICATION

## Functionalization, re-functionalization and rejuvenation of ssDNA nanotemplates†

Ming-Yu Lin,<sup>ab</sup> Fu Han Ho,<sup>c</sup> Chung-Yao Yang,<sup>d</sup> J. Andrew Yeh<sup>d</sup> and Yuh-Shyong Yang<sup>\*a</sup>

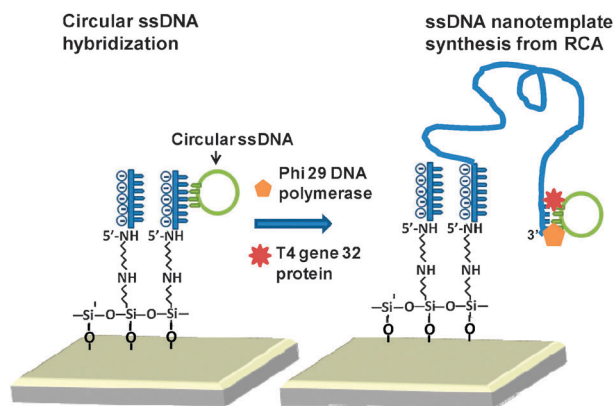
Received 2nd February 2012, Accepted 20th March 2012

DOI: 10.1039/c2cc30748k

Single-stranded DNA (ssDNA) with repetitive sequence was demonstrated to be a versatile nanotemplate for introducing biological activity in a self-assembled manner. Re-functionalization and rejuvenation of the ssDNA nanotemplate were achieved under mild biological conditions without using high temperature and strong alkaline treatment to denature DNA.

Nowadays, DNA is used as more than just a carrier of genetic codes of life; it also serves as a generic building block for nanostructures.<sup>1</sup> The Watson–Crick base-pairing strategy has been applied to construct artificial branched DNA tiles and a complex periodic 2D lattice from the tiles.<sup>2</sup> The next step in DNA nanotechnology is to investigate the possibility of fabricating materials with practical uses, precise positioning,<sup>3</sup> and integrating DNA nanostructures into more complex devices.<sup>4</sup> The unparalleled self-recognition properties of DNA-based nanostructures can provide flexibility and convenience for bottom-up construction of delicate materials with high controllability and precision.<sup>5</sup> Functionalized nanostructures for the self-assembling attachment of various molecules such as proteins,<sup>6</sup> metal nanoparticles,<sup>7</sup> and carbon nanotubes<sup>8</sup> would be very useful in the development of nano-electronics, biosensors, and programmable/autonomous molecular machines.<sup>9</sup> In this study, we *in situ* assembled long ssDNA with repetitive sequence on a silicon-based substrate. The ssDNA nanostructure was used as a nanotemplate and functionalized with enzyme activity. The bioactive ssDNA nanotemplates could be re-functionalized with another enzyme activity and rejuvenated without high temperature and strong alkaline treatment.

*In situ* synthesis of self-assembled ssDNA nanotemplates on silicon-based materials was achieved following the formation of a self-assembled monolayer (SAM), circular ssDNA hybridization,



**Scheme 1** *In situ* synthesis of an ssDNA nanotemplate on a silicon-based substrate. The 18 n.t. DNA primer was covalently immobilized on the substrate as an SAM layer. The circular ssDNA served as a template for the synthesis of a long and periodic ssDNA nanotemplate. Phi29 DNA polymerase not only served as a molecular machinery for construction of ssDNA nanostructures, but was also a gate keeper to proofread the DNA sequence during RCA. T4 gene 32 protein was the ssDNA-binding protein that stabilized the newly synthesized ssDNA and prevented it from re-hybridizing with the circular RCA template.

and rolling circle amplification (RCA) (Scheme 1).<sup>10</sup> For the applications of DNA nanotemplates to biosensors, bioreactors and other devices, one end of the ssDNA must be immobilized on their surfaces in order to control the positioning of the nanotemplate on the sensing/reacting area and to discriminate non-specific binding molecules in the washing step. The synthesis of ssDNA nanotemplates on silicon-based material was initiated by *in situ* aptamer recognition. Our purpose was to assemble ssDNA nanostructures functionalized with programmable biological activities *in situ*, and the use of circular ssDNA with RCA provided an additional regulation mechanism for the synthesis of the ssDNA nanotemplates.

As depicted in Scheme 1, the DNA primer labeled with  $-NH_2$  at its 5'-end was immobilized on a 3'-aminopropyl triethoxysilane (APTES) and glutaraldehyde-bridged glass substrate through silanization. Circular ssDNA was the template for DNA synthesis and was prepared following the ligation of the 5'-phosphated platelet-derived growth factor (PDGF) aptamer.<sup>11</sup> PDGF acted as a conformation switch on the DNA aptamer to induce its circularization catalyzed by ligase. Alternatively, a circular ssDNA could be provided directly as a template or from

<sup>a</sup> Institute of Molecular Medicine and Bioengineering, National Chiao Tung University, Hsinchu, Taiwan. E-mail: ysyang@mail.nctu.edu.tw; Fax: +886-3-5729288; Tel: +886-3-5731983

<sup>b</sup> Instrument Technology Research Center, National Applied Research Laboratories, Hsinchu, Taiwan

<sup>c</sup> Graduate Institute of Applied Science and Technology, National Taiwan University of Science and Technology, Taipei, Taiwan

<sup>d</sup> Institute of NanoEngineering and MicroSystems, National Tsing Hua University, Hsinchu, Taiwan

† Electronic supplementary information (ESI) available: Materials and methods, time-dependent synthesis and diagrams for re-functionalization and rejuvenation of ssDNA nanotemplates. See DOI: 10.1039/c2cc30748k

ligated padlock for biosensing purposes.<sup>12</sup> The circular ssDNA hybridized with immobilized primers, and RCA was initiated following the addition of Phi29 DNA polymerase and the T4 gene 32 protein to produce an ssDNA repetitive sequence. The sequence and length of each repeat on the ssDNA nanotemplate were determined by the sequence of circular ssDNA. Hence, the sequence of the ssDNA nanotemplate is pre-programmable through the design of the circular ssDNA. In this study, each repeat of the ssDNA nanotemplate contained 96 nucleotides (n.t.) that serve as a probe binding site for incorporation of specific functions (Fig. S1, ESI†). Following nine or more RCA cycles, the overall secondary structures of the ssDNA nanotemplate were predicted to uniformly contain double-hairpins as shown in Tables S1 and S2 (ESI†). This indicates that the long and periodic ssDNA can be very suitable to serve as a nanotemplate for homogeneously harboring the expected entity. The predicted secondary ssDNA structures were consistent with the ssDNA nanostructure monitored by AFM (Fig. S2–S4, ESI†). Only two major shapes (globular and dumbbell) were observed following long RCA reaction time (90 and 120 min) and the lowest height (about 7 nm) was equivalent to that of the predicted secondary ssDNA structure (Fig. S1, ESI†).

Incorporation of biomolecules into the immobilized ssDNA nanotemplate can be achieved through the adaptor that would self-assemble on the RCA-synthesized ssDNA nanotemplate (Fig. S5A, ESI†). The adaptor contained a presenter (enzyme), streptavidin (covalently bound to the presenter), biotin, and the 15 n.t. long biotin-labeled DNA probe. This design allows the presenter (enzyme 1) attached to the ssDNA nanotemplate to be easily replaced with another presenter (enzyme 2) covalently bound to streptavidin (Fig. S5B, ESI†) through the exchange between immobilized and free streptavidin on the biotinylated probe. The longer DNA nanotemplate could accommodate more DNA probes and thus the time-dependent synthesis of the bioactive DNA nanostructure could be monitored by measuring the activity of the enzyme attached to the DNA biotinylated probe. Activities of HRP and AP were determined through reactions with colorimetric reagents as described in ESI†. As shown in Fig. 1A, horseradish peroxidase (HRP) activity could be observed following the addition of streptavidin conjugated peroxidase (Strep–HRP) only when the adapter binds tightly to the ssDNA nanotemplate and was increased with longer RCA reaction time. This observation was consistent with the growth of the ssDNA nanostructure observed by scanning probe microscopy (Fig. S2–S4, ESI†). In addition, HRP activity on the ssDNA nanotemplate was also dependent on the concentration of aptamers that were added to initiate ssDNA synthesis (Fig. S6, ESI†). These results indicated that the length and the number of the immobilized ssDNA nanotemplates could be regulated through reaction time and aptamer concentration, respectively, to host various amounts of enzyme activities.

The enzyme integrated onto the ssDNA nanotemplate can be replaced with another biological entity as illustrated in Fig. S5A and B (ESI†). This scheme demonstrated experimentally that the HRP originally functionalized on the DNA nanotemplate was gradually replaced with alkaline phosphatase conjugated with streptavidin (Strep–AP). About  $83 \pm 4.2\%$  of HRP originally functionalized on DNA nanotemplates was replaced with alkaline phosphatase (AP) following 700 nM

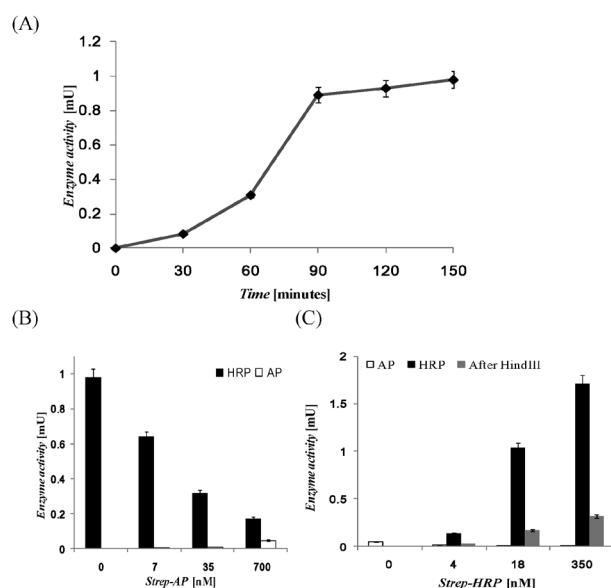


**Fig. 1** Functionalization and re-functionalization of immobilized ssDNA nanotemplates. (A) Time-dependent functionalization of the ssDNA nanotemplate with peroxidase activity. A biotin-labeled DNA probe (130 pmol) was added into reaction mixture at desired time following the initiation of RCA reaction. The ssDNA nanotemplate was washed with washing buffer three times to remove the unbound biotin-labeled probe. Strep–HRP (0.34 pmol) was then mixed with the ssDNA nanotemplate followed by another three-time washing buffer wash to remove any unbound peroxidase activity. Each streptavidin entity contains multiple HRP. (B) Re-functionalization of the bioactive DNA nanotemplate. HRP activity on the DNA nanotemplate was replaced with AP activity with various concentration of Strep–AP. There are 2 streptavidin conjugating with 1 AP. (C) Replacement and removal of enzyme activities on the ssDNA nanotemplate. Alkaline phosphatase was replaced with peroxidase activities on the DNA nanotemplate and the peroxidase activity was further removed following treatment with restriction enzyme, HindIII. The enzyme activities were determined as described in the Method section. The error bars indicate the 5% error value over five separate glass substrates at each desired time for time-dependent experiments, and four separate glass substrates for re-functionalization measurement experiments.

Strep–AP competitive treatment. A concentration-dependent change of enzymatic activities was observed (Fig. 1B), which indicated the competition between streptavidin binding enzymes (Strep–HRP and Strep–AP) with the biotinylated probe. Similar results were obtained when Strep–HRP was used to replace AP originally functionalized on the DNA nanotemplate (Fig. 1C). About  $88.4 \pm 2\%$  of AP originally functionalized on DNA nanotemplates was replaced with HRP following 350 nM Strep–HRP competitive treatment. With proper mixtures of streptavidin-conjugated enzymes, either a single or a variety of enzyme activities can be functionalized on the ssDNA nanotemplates. To further confirm that all the enzyme activities observed exclusively came from the immobilized ssDNA nanotemplate, the DNA nanotemplate was removed by a DNA restriction enzyme, HindIII (restriction site is shown in Fig. S1 and S5A, ESI†), from the glass substrate. In the absence of the ssDNA nanotemplate, the HRP activity was eliminated (Fig. 1C).

Results shown in Fig. 1B and C indicated that, by using different combinations of the streptavidin–enzyme complex

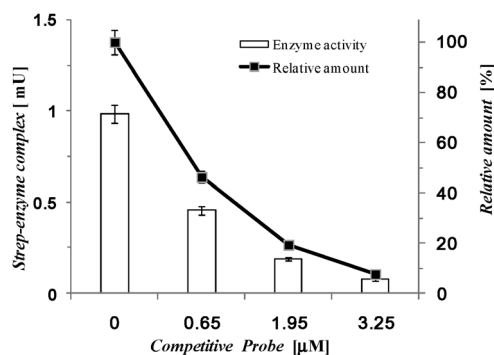


**Fig. 2** Rejuvenation of functionalized ssDNA nanotemplates. HRP activity following rejuvenation of the functionalized ssDNA nanotemplate with recovery DNA was measured. Recovery DNA (0, 0.65, 1.95, 3.25 μM) was added sequentially to the functionalized ssDNA nanotemplate that was functionalized with the 21 n.t. 3'-extended probe at 37 °C for 60 min. Following three-time rinsing with washing buffer, Strep-HRP was added to evaluate any probes left on the nanotemplate. The error bars indicate the 5% error value over three separate glass substrates.

(such as Strep-HRP, and Strep-AP in this study), a tunable functionalization of substrates with nanostructures can be manipulated. In addition, various amounts of biological activities can also be controlled. It should be noted that an immobilized biotin-streptavidin complex can be readily exchanged with other free streptavidin.<sup>13</sup> In this study, each AP entity contained 2 streptavidin conjugates (#S2890, Sigma, USA), while there were multiple HRP with each streptavidin (#S2438 from Sigma, USA). Therefore, for every binding site on the ssDNA nanotemplate, there can be only one AP but may contain multiple HRP through streptavidin and biotin interaction. Thus, as shown in Fig. 1B and C, it appeared that significantly more HRP was incorporated into the ssDNA nanotemplates than AP. About 0.98 mU (1.97 fmol) of HRP and 0.05 mU (0.17 fmol) of AP were incorporated into the free ssDNA nanotemplate, respectively. This result indicated that each binding site of the ssDNA nanotemplate could accommodate about 11.6 HRP, which was consistent with the Strep-HRP used in this study. Competition between AP and HRP on the ssDNA nanotemplate also showed that 0.81 mU (1.63 fmol) of HRP was replaced by 0.05 mU (0.17 fmol) of AP (Fig. 1B), and 0.04 mU (0.15 fmol) of AP was replaced by 1.71 mU (3.43 fmol) of HRP (Fig. 1C).

With proper design of the biotinylated DNA probes, the functionalized ssDNA nanotemplates can be recovered to its unbound state under mild biological conditions as shown in Fig. S7 (ESI†). In this scheme, rejuvenation of the bioactive DNA nanotemplate could be achieved by removing the biotinylated DNA probes on the ssDNA nanotemplate by using a recovery DNA. Such scheme has been demonstrated previously in manipulating closed and open forms of DNA nanodevices.<sup>14</sup> In this study, the recovery DNA contains 21 n.t. that completely complements the biotinylated probe (15 n.t. complementary sequence with the ssDNA nanotemplate and 6 n.t. extended sequence at the 3' end) and is thus thermodynamically more favorable to form a probe-recovery DNA duplex than that of the probe-DNA template. The predicted free-energy changes ( $\Delta G$ ) of the 21 n.t.

biotinylated probe-recovery DNA duplex and biotinylated probe-15 n.t. binding sites of DNA nanotemplates under the experimental conditions (50 mM KCl, 10 mM MgCl<sub>2</sub> at 25 °C) were  $-22.72$  and  $-15.94$  kcal ml<sup>-1</sup> respectively. The 21 n.t. recovery DNA effectively eliminated the peroxidase activity on the DNA nanotemplate, which was found to be dependent on the concentration of recovery DNA (Fig. 2). More than 90% of the HRP activity was removed by 3.25 μM recovery DNA. This result indicated that both the HRP and the DNA probes were taken away from the ssDNA nanotemplate.

We demonstrated that long and periodic ssDNA nanostructures could be prepared on the silicon based substrate and could serve as nanotemplates for self-organized enzymatic activity. Similar procedures can be used to incorporate various other enzymes and biomolecules such as antibodies or receptor proteins to produce specific biological functions on the ssDNA nanotemplate. The nanotemplate could be further manipulated by re-functionalization and rejuvenation *in situ* under mild and biologically compatible conditions and could be a versatile tool as tunable functional materials to produce desired biological functions for biosensors, bioreactors, and other applications.

This work was supported by National Science Council (NSC 101-2923-B-009-001) and MOE-ATU Program to Y.-S. Yang.

## Notes and references

- 1 F. A. Aldaye, A. L. Palmer and H. F. Sleiman, *Science*, 2008, **321**, 1795.
- 2 (a) N. C. Seeman, *Nature*, 2003, **421**, 427; (b) C. Lin, Y. Liu, S. Rinker and H. Yan, *ChemPhysChem*, 2006, **7**, 1641; (c) F. A. Aldaye and H. F. Sleiman, *J. Am. Chem. Soc.*, 2007, **129**, 4130; (d) Y. He, T. Ye, M. Su, C. Zhang, A. E. Ribbe, W. Jiang and C. Mao, *Nature*, 2008, **452**, 198; (e) D. Han, S. Pal, J. Nangreave, Z. Deng, Y. Liu and H. Yan, *Science*, 2011, **332**, 342–346.
- 3 (a) G. Maubach and W. Fritzsche, *Nano Lett.*, 2004, **4**, 607; (b) G. Maubach, A. Csaki, D. Born and W. Fritzsche, *Nanotechnology*, 2003, **14**, 546.
- 4 R. M. Stoltenberg and A. T. Woolley, *Biomed. Microdevices*, 2004, **6**, 105.
- 5 H. Hao, N. Lu, Y. Wen, S. Song, Y. Liu, H. Yan and C. Fan, *Adv. Mater.*, 2010, **22**, 4754.
- 6 O. I. Wilner, S. Shiron, Y. Weizmann, Z.-G. Wang and I. Willner, *Nano Lett.*, 2009, **9**, 2040.
- 7 W. Zhao, Y. Gao, S. A. Kandadai, M. A. Brook and Y. Li, *Angew. Chem., Int. Ed.*, 2006, **45**, 2409.
- 8 M. Hazani, R. Naaman, F. Hennrich and M. Kappes, *Nano Lett.*, 2003, **3**, 153.
- 9 H. Yan, S. H. Park, G. Finkelstein, J. H. Reif and T. H. LaBean, *Science*, 2003, **301**, 1882.
- 10 (a) W. Zhao, M. M. Ali, M. A. Brook and Y. Li, *Angew. Chem., Int. Ed.*, 2008, **47**, 6330; (b) P. J. Paukstelis and A. D. Ellington, *Proc. Natl. Acad. Sci. U. S. A.*, 2008, **105**, 17593; (c) Z. Cheglakov, Y. Weizmann, A. Braunschweig, O. Wilner and I. Willner, *Angew. Chem.*, 2008, **12**, 132.
- 11 J. Sun, H. Zhou, Y. Jin, M. Wang, Y. Li and N. Gu, *ChemPhysChem*, 2008, **9**, 1847.
- 12 [http://www.sigmaaldrich.com/catalog/ProductDetail.do?lang=en&N4=P0114SIGMA&N5=SEARCH\\_CONCAT\\_PNO|BRAND\\_KEY&F=SPEC](http://www.sigmaaldrich.com/catalog/ProductDetail.do?lang=en&N4=P0114SIGMA&N5=SEARCH_CONCAT_PNO|BRAND_KEY&F=SPEC).
- 13 G. R. Broder, R. T. Ranasinghe, C. Nylon, H. Morgan and P. L. Roach, *Anal. Chem.*, 2011, **83**, 2005.
- 14 B. Yurke, A. J. Turberfield, A. P. Mills, F. C. Simmel and J. L. Neumann, *Nature*, 2000, **406**, 605.